ARL-TR-7501 ● Oct 2015

US Army Research Laboratory

Friction Mapping as a Tool for Measuring the Elastohydrodynamic Contact Running-in Process

by Stephen Berkebile and Nikhil Murthy

NOTICES

Disclaimers

The findings in this report are not to be construed as an official Department of the Army position unless so designated by other authorized documents.

Citation of manufacturer's or trade names does not constitute an official endorsement or approval of the use thereof.

Destroy this report when it is no longer needed. Do not return it to the originator.

ARL-TR-7501 ● OCT 2015

US Army Research Laboratory

Friction Mapping as a Tool for Measuring the Elastohydrodynamic Contact Running-in Process

by Stephen Berkebile
Vehicle Technology Directorate, ARL

Nikhil Murthy
Engility, Chantilly, VA

REPORT DOCUMENTATION PAGE

Form Approved
OMB No. 0704-0188

1. REPORT DATE *(DD-MM-YYYY)*	2. REPORT TYPE	3. DATES COVERED (From - To)
October 2015	Final	1 January–30 June 2015

4. TITLE AND SUBTITLE
Friction Mapping as a Tool for Measuring the Elastohydrodynamic Contact Running-in Process

5a. CONTRACT NUMBER

5b. GRANT NUMBER

5c. PROGRAM ELEMENT NUMBER

6. AUTHOR(S)
Stephen Berkebile and Nikhil Murthy

5d. PROJECT NUMBER

5e. TASK NUMBER

5f. WORK UNIT NUMBER

7. PERFORMING ORGANIZATION NAME(S) AND ADDRESS(ES)
US Army Research Laboratory
ATTN: RDRL-VTP
Aberdeen Proving Ground, MD 21005

8. PERFORMING ORGANIZATION REPORT NUMBER
ARL-TR-7501

9. SPONSORING/MONITORING AGENCY NAME(S) AND ADDRESS(ES)

10. SPONSOR/MONITOR'S ACRONYM(S)

11. SPONSOR/MONITOR'S REPORT NUMBER(S)

12. DISTRIBUTION/AVAILABILITY STATEMENT
Approved for public release; distribution is unlimited.

13. SUPPLEMENTARY NOTES

14. ABSTRACT
Elastohydrodynamically lubricated gear and bearing contacts typically demonstrate a period of wear called “running-in” when they are first put into service, during which time the friction coefficient of the 2 mating surfaces drops rapidly. The running-in process depends on numerous contact conditions and material properties. These dependencies are important to understand, since running-in has lasting consequences for the operation, efficiency, and failure conditions of the contact. In this report, we demonstrate friction mapping as a method to characterize the running-in process, using a high-speed ball-on-disc tribometer to measure the coefficient of friction as a function of entrainment velocity and slip for different contact histories. We observe that the final state friction coefficient and surface morphology, once the running-in process is complete, does not depend significantly on the ramp direction, nor on the particular range for those measured here. However, the running-in occurs at different rates and at different entrainment velocity and slip values, depending on the ramp direction and extent of mapping range.

15. SUBJECT TERMS
elastohydrodynamic, lubrication, wear, gears, bearings

16. SECURITY CLASSIFICATION OF:			17. LIMITATION OF ABSTRACT	18. NUMBER OF PAGES	19a. NAME OF RESPONSIBLE PERSON
a. REPORT	b. ABSTRACT	c. THIS PAGE			Stephen Berkebile
Unclassified	Unclassified	Unclassified	UU	36	19b. TELEPHONE NUMBER (Include area code) (410) 278-9547

Contents

List of Figures

List of Tables

INTENTIONALLY LEFT BLANK.

1. Introduction

Elastohydrodynamic lubricated contacts are common in vehicle transmission gears and bearings. The hydrodynamic pressure built up in the lubricant film is sufficient to prevent most contact between the 2 opposing solid surfaces during normal operation, which results in extremely low wear rates and long lifetimes over millions and billions of cycles. Yet even the surfaces of these high-speed components typically demonstrate a period of wear called "running-in" when they are first put into service, especially during start and stop cycles when lower speeds reduce the lubricant film thickness. During this period of running-in, the friction coefficient of the 2 mating surfaces drops rapidly as they become smoother. This polishing effect presumably occurs as asperities from machining of the components are removed or flattened, although other chemical or morphological changes may also be taking place.[1–5]

The running-in process has lasting consequences for the operation, efficiency, and failure conditions of the contact. The efficiency and heat production are directly related to the friction coefficient in a contact, while failure modes, such as micropitting and scuffing, depend more on surface roughness, asperities, and chemical state of the surfaces.[3,6–7] Because the amount of wear, type of wear, and wear rate depends on the lubricant, material, and elements of contact history, such as speed and load, it is essential to gain an understanding of how these factors affect running-in.

With the development of experimental lubricants, materials, and operational geometries, there is a need for methods that quantify running-in and measure its overall effect on performance over a large range of relevant contact conditions. Many studies of running-in have been conducted to look at the change in roughness at a single set of contact conditions and to discover methods to relate the roughness profile analysis quantitatively to friction coefficient change or wear rate.[8–13] Studies that have investigated varying contact conditions, such as slide-to-roll ratio (SRR), load, and entrainment velocity, see a dependence of the running-in wear on the specific conditions.[14–18] However, little information exists on the overall effect of running-in on the friction coefficient over wider ranges of surface velocities and how the contact history determines the amount of running-in.

In this report, we introduce friction mapping as a method to characterize the running-in process. In friction mapping, the friction coefficient is measured and displayed over 2 or more variables of interest. Two variables that are critical to gear and bearing mechanical contacts are entrainment velocity and SRR, or slip.

When the friction coefficient is measured as a function of entrainment velocity, one is essentially changing the film thickness with changing velocity, replicating the well-known Stribeck curve with the associated changes in the lubrication regime. When the slip is varied, the shear within the contact changes, increasing the contact severity and power generation with increasing sliding velocity. Björling et al. have used friction mapping with entrainment velocity and slip to study friction coefficient, surface roughness, lubricant viscosity and type, surface material, and lubrication regime.[19–22] By mapping over these variables during the running-in process, we can also study the contact history that cause running-in and the friction coefficient that one can expect during and after the running-in process.

2. Methods and Procedures

The running-in measurements were conducted using the WAM14 Wedeven Associates Machine (Wedeven Associates Incorporated) ball-on-disc tribometer at the US Army Research Laboratory. The WAM14 is capable of operating at high speeds and loads with precise control over the contact conditions. The WAM14 allows for independent control over ball and disc velocities, the vertical contact load, oil flow rate, and specimen temperature. Experiments are run on a specified track diameter defined by the location of the ball and disc contact so that several fresh tracks can be used on a single side of a disc. The traction coefficient, also known as the friction coefficient, is measured from the force exerted on the ball by several load cells attached to a support table suspended on air bearings. The ball-on-disc system is shown in Fig. 1.

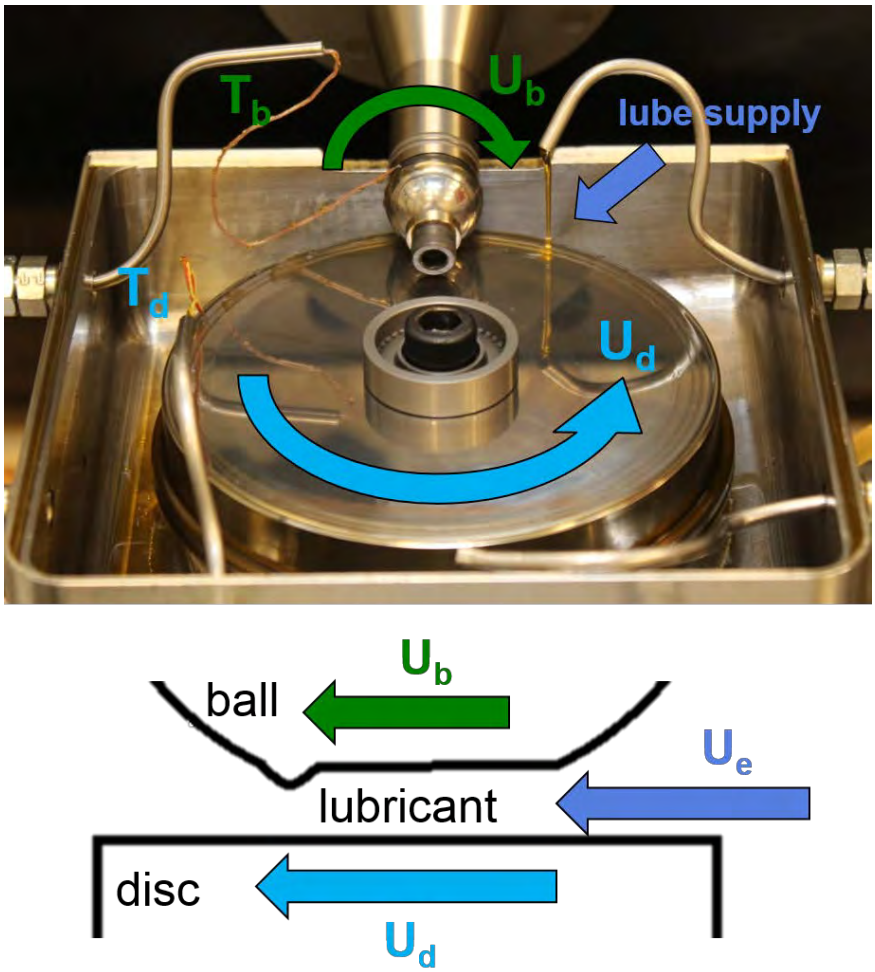

Fig. 1 WAM14 ball-on-disc tribometer (top) with ball and disc velocity, U_b and U_d, and temperature measurements, T_b and T_d, and schematic of the contact zone with corresponding ball, disc, and entrainment U_e velocities (bottom)

In the photograph (top) and the schematic (bottom) of Fig. 1, the linear surface velocities of the ball and the disc are given as U_b and U_d, respectively. The temperatures are measured using thermocouples placed in contact with the ball and disc surface, labeled T_b and T_d, respectively.

The entrainment velocity U_e is the average of the ball and disc velocities, U_b and U_d, at the contact zone:

$$U_e = \frac{U_b + U_d}{2}. \tag{1}$$

The sliding velocity is the relative velocity between the 2 contacting surfaces and calculated from the ball velocity less disc velocity as

$$U_s = U_b - U_d. \tag{2}$$

The relationship between sliding velocity and entrainment velocity is given either as the SRR ratio,

$$SRR = \frac{U_s}{U_e}, \tag{3}$$

or as the slip in percentage

$$Slip = \frac{U_s}{U_e} * 100\% . \tag{4}$$

We have chosen to use slip throughout this report.

The friction coefficient has been measured as a function of entrainment velocity and slip as they vary with contact history and time. Various ranges of velocities and several directions of ramping the relative velocities have been chosen to demonstrate the similarities and differences that are seen to depend on the particular choice of friction mapping procedure. A plot of the entrainment velocity, U_e, and slip percentage is displayed for one of the friction mapping procedures in Fig. 2. In this case, the entrainment velocity is ramped linearly from 16 to 0.35 m/s over 90 s, held for 10 s at 0.35 m/s, and ramped back to 16 m/s at a slip of 0.03%. Once this ramp is complete, the slip is increased one step, held for 10 s, then the ramp is repeated. This procedure continues for all slip values shown in Fig. 2.

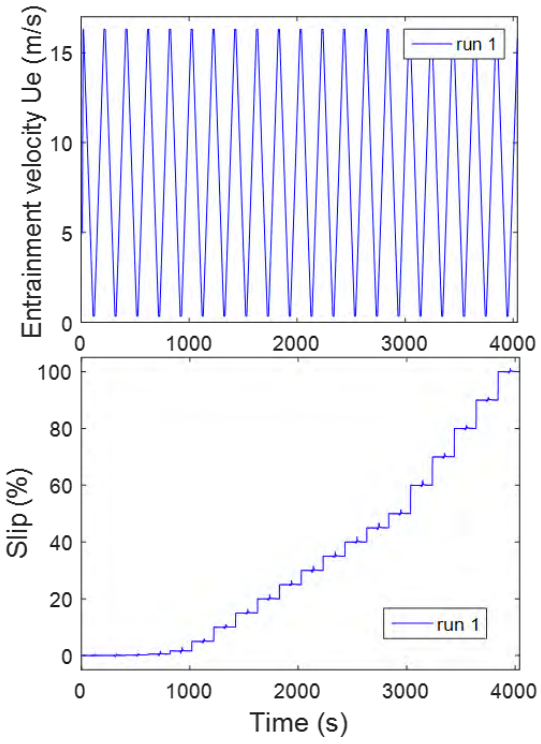

Fig. 2 Simultaneous measurements of the actual entrainment velocity (top) and slip (bottom) during the friction mapping procedure in which entrainment velocity is ramped while slip is stepped by control of disc and ball velocities

An example of the measured friction coefficient, also known as the traction coefficient, plotted as a function of entrainment velocity and slip is shown in Fig. 3. The upper plot displays the data as a surface plot while the lower plot displays the same data as a contour plot. The surface plot is shown because it allows a rapid recognition of 3 main areas and their relationship to each other. Along the entrainment velocity direction, the friction values correlate to classic Stribeck curves with high friction coefficient at low velocity dropping sharply to a flat region at higher velocity. Along the slip axis, traction curves, often used for bearing measurements, can be recognized. Following the analyses in Björling et al.[21] and Habchi et al.[23], we can divide the plot into 3 primary friction regimes: 1) the mixed lubrication regime in yellow/green at low entrainment velocity, 2) the linear regime in the darkest blue at low slip values, and 3) the thermoviscous regime, characterized by the mid-blue plateau over most of the plot range. These regimes are displayed in the contour plot of Fig. 3. Contour plots will be used throughout this report because they allow for a direct visual comparison between different friction maps and a clear depiction of the differences between maps when they are subtracted from each other. All friction maps use contours separated by a friction coefficient of 0.002 with every 0.01 labeled, while differences between friction maps use contours of 0.0005 with every 0.002 labeled. Before plotting and for plot subtraction purposes, the friction coefficient values are mapped onto a grid of entrainment velocity and slip (see upper plot of Fig. 3 for the grid) using a natural neighbor interpolation procedure.

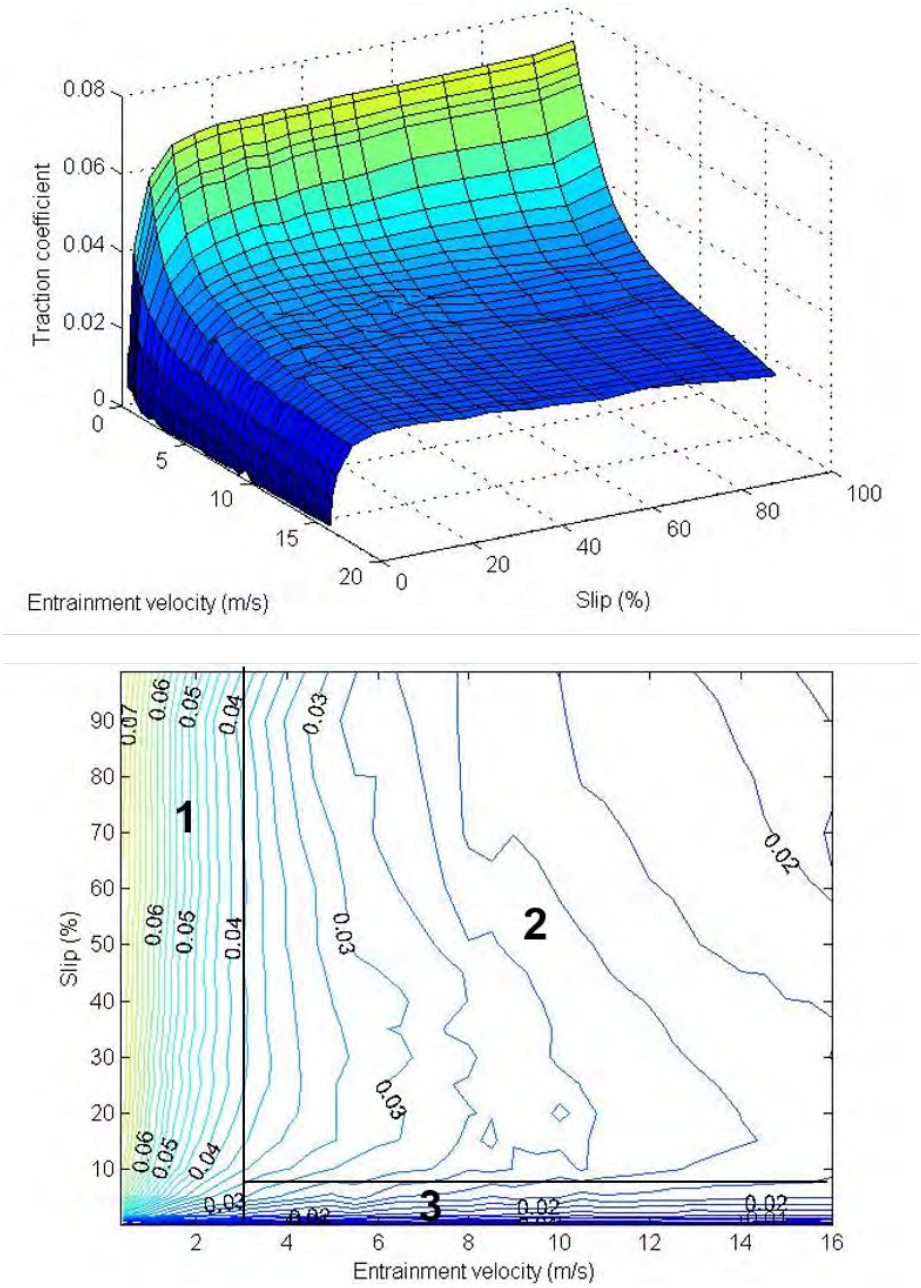

Fig. 3 Three-dimensional surface plot of the traction coefficient (friction coefficient) as a function of entrainment velocity and slip (top) and the same data plotted as a contour plot divided into friction regimes (bottom)

In all, 4 friction mapping procedures were used; the entrainment velocity is ramped in 3 of the procedures, and the slip is ramped in one. The nonramped value is either stepped or held constant. The details of ramp ranges, ramp times, and steps for the 4 mapping procedures are given in Table 1. These procedures are graphically depicted in Fig. 4. For measuring the running-in, the particular mapping procedure was repeated numerous times on a single fresh track. Throughout the report, a fully completed procedure that produces a friction map will be referred to as a map, friction map, or run when several maps are completed in sequence. When the difference in the friction coefficient from run to run was 0.002 or less over the entire map except for a few grid points and 0.003 or less over all grid points, the running-in process was considered to be complete. For each step, ramped entrainment velocity always begins at 16 m/s and ramped slip begins at 0%. Because the ramp moves in both directions, there are essentially 2 maps created, one for increasing ramped value and one for decreasing ramped value. In this report, the friction maps use the first portion of the ramp (i.e., decreasing entrainment velocity or increasing slip).

Table 1 Friction mapping procedures

ID	Procedure	Ramped value range	Ramp time	Stepped values	Time spent <2 m/s per map
A	Ramp U_e, step slip	16.3 m/s ↔ 0.35 m/s	90 s	Slip –0.02% → –100%[a,b]	650 s
B	Ramp U_e (reduced range), step slip	16.3 m/s ↔ 2.5 m/s	90 s	Slip –0.02% → –100%[a,b]	0 s
C	Ramp slip, step U_e	–0.02% ↔ –100% [a]	90 s	U_e 16 m/s → 0.35 m/s[c]	1,800 s
D	Ramp U_e, constant slip	16 m/s ↔ 0.35 m/s	90 s	Slip constant at 95%	487.5 s

[a] Negative slips indicate that the disc has a higher surface velocity than the ball at the contact point.
[b] The full list of slips are –0.02, –0.06, –0.18, –0.54, –1.62, –5, –10, –15, –20, –25, –30, –35, –40, –45, –50, –60, –70, –80, –90, and –100%.
[c] The full list of entrainment velocities are 16, 15, 14, 13, 12, 11, 10, 9, 8, 7, 6, 5, 4, 3.5, 3, 2.5, 2, 1.5, 1.25, 1.1, 0.95, 0.80, 0.65, 0.50, and 0.35 m/s.

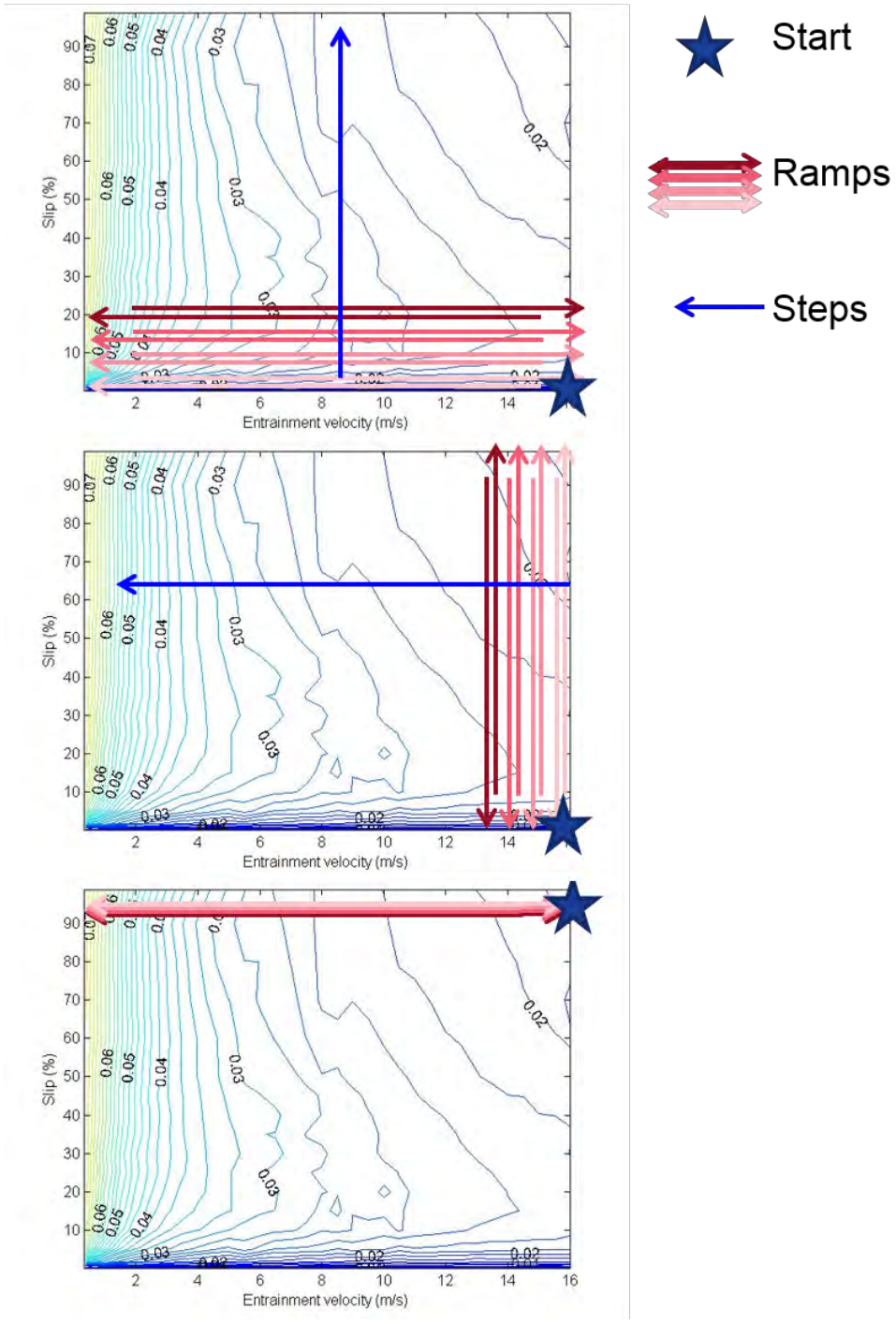

Fig. 4 Depiction of ramp and step procedures on a set of generic friction mapping data: ramped entrainment velocity with stepped slip (top), ramped slip with stepped entrainment velocity (center), ramped entrainment velocity with constant slip (bottom)

Materials and contact parameters used throughout the measurements in this report are given in Table 2. The discs and balls were cleaned with petroleum ether and then acetone in an ultrasonic bath before use. Before each sequence of maps, conditions of pure rolling (slip = 0%) were found at an entrainment velocity of U_e = 8 to 10 m/s. The lubricant was supplied at 100 °C and the disc was brought to 126 °C before mapping to reproduce typical aerospace gear and bearing operating temperatures.

Table 2 Materials and contact parameters

Parameter	Value	Comments
Disc material	AISI 9310 steel	Circumferential grind, initial $Sa \approx 100$ nm
Ball material	AISI 9310 steel	Tumbled finish, initial $Sa \approx 200$ nm, diameter $d = 20.6$ mm
Contact load	200 N	Corresponds to a maximum Herztian stress of 1.63 GPa
Lubricant	DOD-PRF-85734	Aeroshell 555
Lubricant supply temperature	100 °C	Lubricant viscosity @ 100 °C is 5 cSt
Initial disc temperature	126 °C	Lubricant viscosity @ 120 °C is 3 cSt

All surface roughness measurements were conducted using a Zeiss LSM700 laser scanning confocal microscope using a 50× objective with a numerical aperture of 0.95 and a laser wavelength of 405 nm. The 3-dimensional (3-D) roughness values were calculated according to ISO 25178[24] from an area 125 by 1300 μm.

3. Results and Discussion

Various friction mapping procedures have been used to observe and quantify the sensitivity of running-in wear to particular contact histories with similar total contact conditions. The detailed list of procedures is given in Table 1. The effects that will be evaluated throughout this section are those of the mapping direction, the exclusion of the mixed lubrication regime, and limiting operation to simulate a single gear mesh point. First, the details of changes that occur from map to map with repetition are presented and discussed using the mapping procedure in which entrainment velocity is ramped over the full range (procedure A). Next, the temperatures due to frictional heating during the mapping procedure are discussed. The mapping procedure A is then compared to mapping procedure B over a reduced range of entrainment velocity. The results from a contrasting mapping procedure C in which slip is ramped are then presented and compared to procedure A. A fourth procedure (procedure D) is then presented that corresponds to a single point along the face of a gear tooth in a spur gear. Finally, the surface topology is compared among different mapping procedures after the running-in processes are largely complete.

3.1 Change in Friction with Operational Time: Ramp U_e, Step Slip

Friction maps collected using procedure A (ramp U_e, step slip) are shown in Fig. 5. The maps, labeled run 1 to run 5, have been measured in sequence on the same track during the same day, while run 6 has been measured the following day on the same track. Each of the maps shows the same basic features as the example given in Fig. 3. The friction coefficient is highest at low entrainment velocity with a sharp decrease in friction over nearly all slip values with increasing entrainment velocity (mixed lubrication regime). The friction coefficient also increases from zero slip to low slips over all entrainment velocities (linear regime) and, with increasing slip, the friction coefficient transitions into a large, relatively flat region that dominates the map at a higher entrainment velocity and slip (thermoviscous regime). Notably, the overall friction coefficient decreases from run 1 to run 3 with little change from run to run between runs 3 and 5. A sixth run was made the next day to see if the friction coefficient changed after a 15-h period over which the sample was allowed to cool to room temperature and was then heated again for the test. As evident in Fig. 5, no difference is seen between run 5 on the previous day and run 6 on the next day.

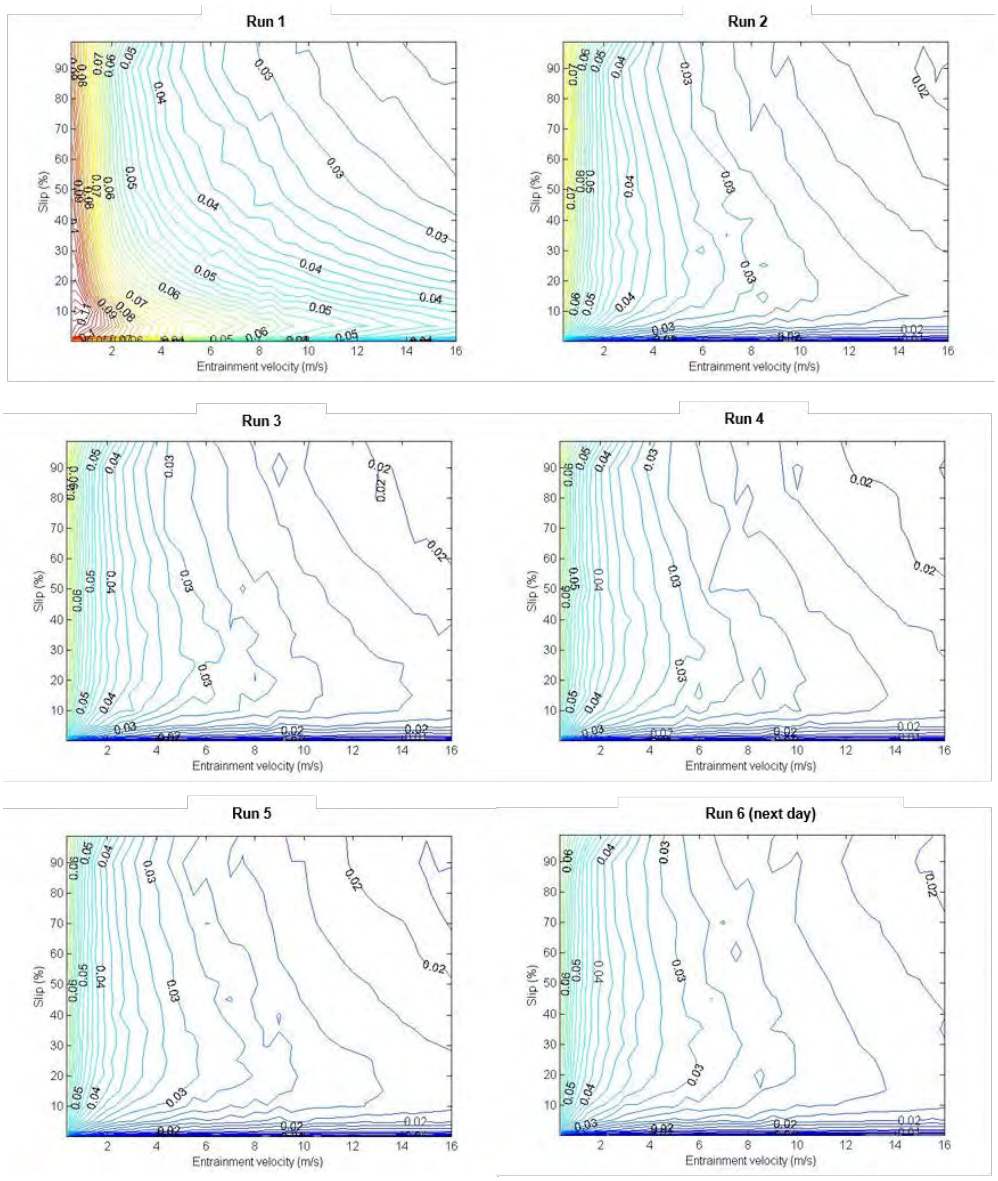

Fig. 5 Subsequent friction maps measured on a single track using the ramp U_e, step slip procedure

The changes in the friction coefficient from run to run can be best seen when the friction maps are subtracted from each other. In Fig. 6, the differences have been taken between each of the subsequent runs and between runs 1 and 5. The decrease in friction is especially large between runs 1 and 2. The difference is concentrated in the mixed lubrication regime and the area of low slip in which the linear regime appears to grow from run 1 to run 2. From runs 2 to 3 and runs 3 to 4, no change is seen except in the mixed lubrication region where friction continues to decrease with each run, albeit at a much reduced rate. After run 4, no more change is observed, as evidenced by runs 4 and 5, having friction coefficients throughout the entire map that are within 0.002 of each other.

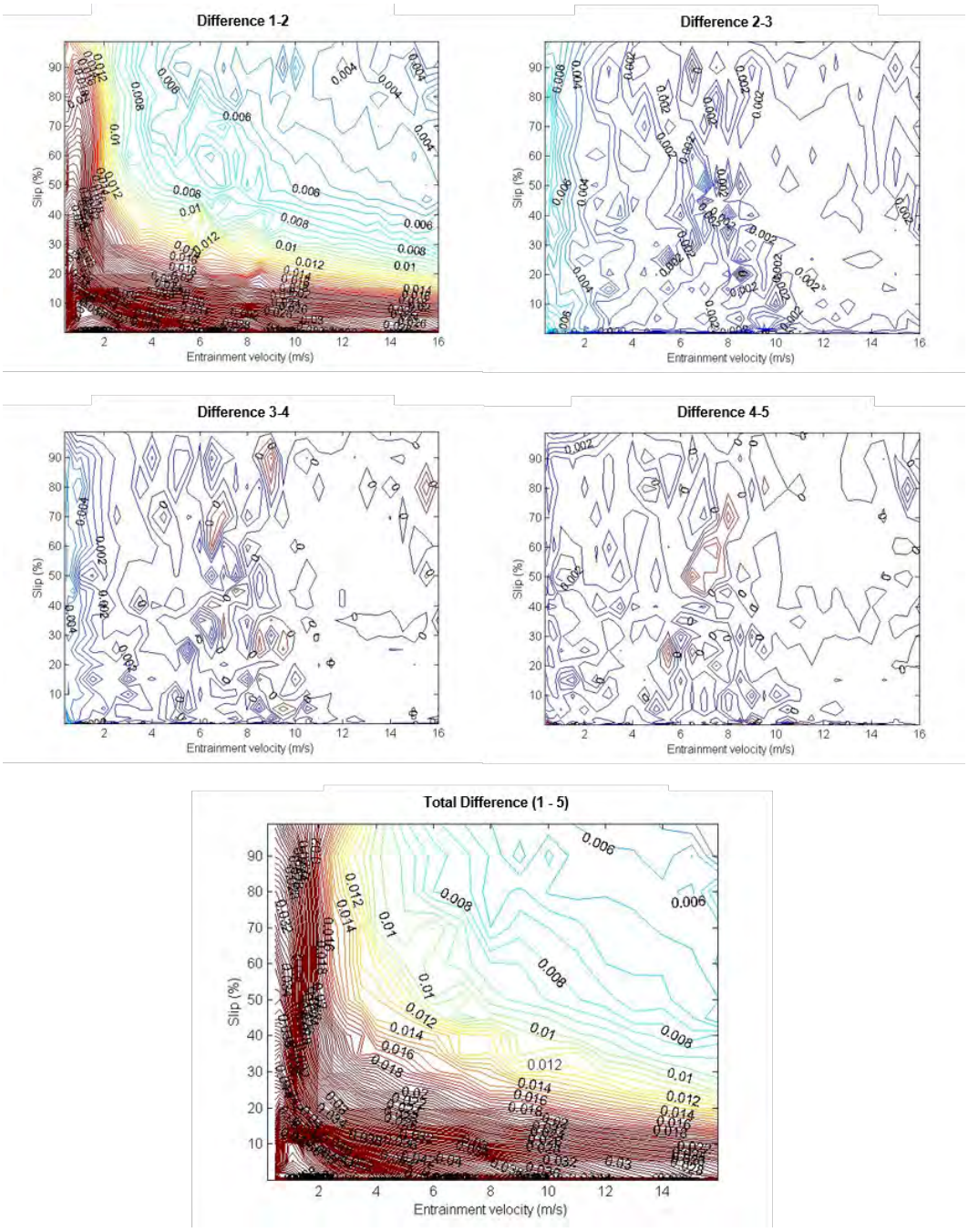

Fig. 6 Difference plots between the friction maps of Fig. 5 subtracting subsequent runs (run 2 from run 1, and so on) and the total difference (run 5 from run 1)

The difference between runs 1 and 5 in Fig. 6 is the total change from the first run until running in wear is complete. Although changes in friction occur over all values of the frictional map, they are concentrated at low entrainment velocities and at low slips. As most of this running-in wear occurs during run 1, it can be expected that the amount of surface polishing is different throughout the entire measured ranges of the friction map. The portions of the friction map measured at a later time experience a smoother surface, essentially producing a measure of the running-in as slip is stepped from 0% to 100%. For this reason, the large change is seen at the lowest slip values because the freshest surface is measured in this region during the first run. As the first mapping procedure continues, running-in still occurs throughout the entire slip range of the map because of the large differences in the friction coefficient in the mixed lubrication regime at low entrainment velocity. The friction coefficient in the thermoviscous regime at higher slip and entrainment velocity is clearly less sensitive to the running-in process, as a total difference of only 0.006 is observed even as differences of 0.03 are occurring in the mixed regime.

3.2 Effect of Running-in on Frictional Heating

The temperature of the disc and ball has been measured during the friction mapping procedure A in the previous section. The temperature during runs 1 and 6 is displayed in Fig. 7 below their corresponding entrainment velocity ramps and slip steps. The disc begins at a temperature of 126 °C, determined by the active heater element, and the ball at around room temperature, 25 °C. When the mapping procedure begins, the ball temperature quickly increases to around 75 °C, and the disc decreases slightly because of the oil supply temperature of 100 °C and cooling from windage. As the slip is increased to values above a few percent, the disc temperature increases slightly, and the temperature of the ball increases sharply, finally ending at a final average temperature of 115 °C. Both temperatures display an oscillation that corresponds to the entrainment velocity ramp. The temperatures increase with high entrainment velocity and decrease with low entrainment velocity, as shown by the red and green guide lines in Fig. 7.

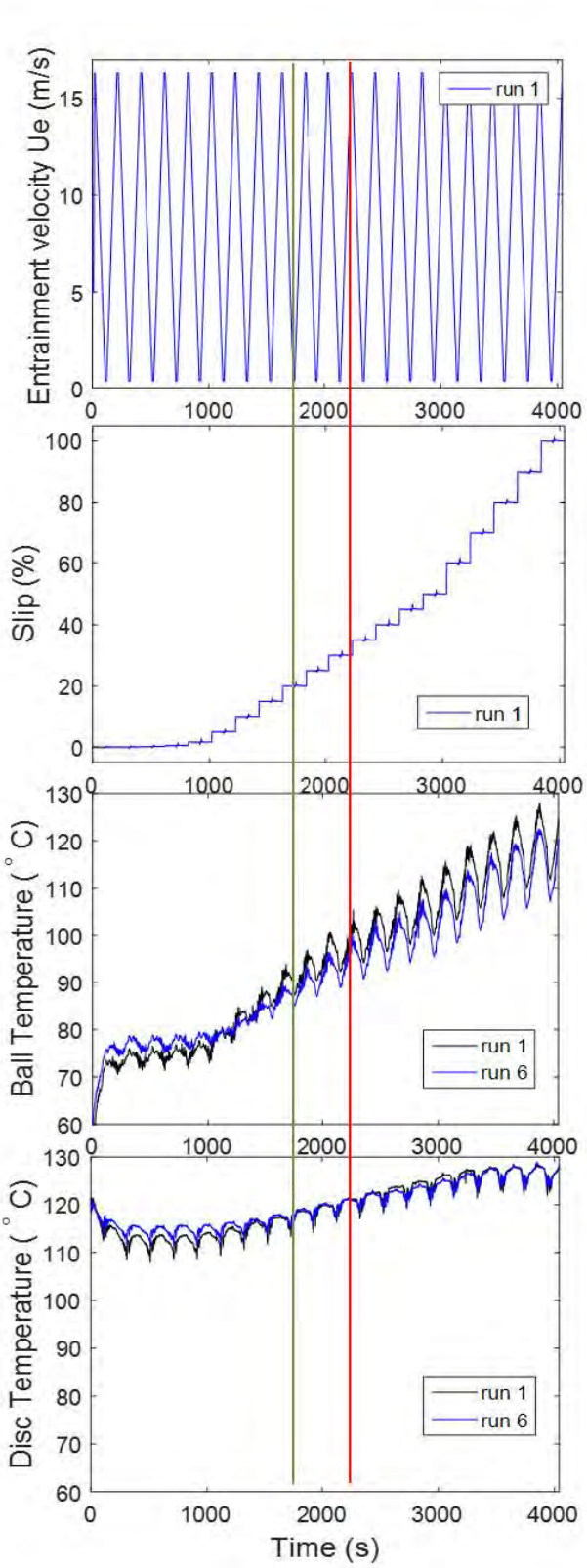

Fig. 7 Simultaneous measurements of entrainment velocity (top), slip (upper center), ball temperature (lower center), and disc temperature (bottom) during the friction mapping procedure in which entrainment velocity is ramped while slip is stepped

The temperature plots demonstrate that most of the heating occurs at higher slips and higher entrainment velocity. The frictional heat dissipation is linearly dependent on the friction coefficient and sliding velocity and will be greatest in areas of high sliding and high friction. At low slip, both friction coefficient and sliding are low, leading the ball to be heated primarily by contact with the lubricant and disc. At higher slip, the friction varies by a factor of 4 over the entrainment velocity range, but the sliding velocity varies by a factor of 40 and dominates the temperature rise. This difference in heating power can be seen in the small effect that running-in (and change in friction) has on the temperature throughout the mapping procedure, as evidenced by the small difference in temperature between runs 1 and 6.

3.3 Comparing Range

To determine the importance of the mixed lubrication regime in the running-in process, friction mapping was conducted over a reduced range using the ramp U_e, step slip procedure B. In the upper 2 graphs of Fig. 8, the first (run 1) and last (run 4) runs are displayed for the reduced range. A comparison to Fig. 5 reveals them to be nearly identical to the friction maps of the full range measurements of procedure A. Likewise, the difference between the first and last run of procedure B displayed in the lower-left graph of Fig. 8 is similar to that of the larger range of procedure A in Fig. 6 over the common range measured. The changes in friction coefficient observed for the reduced range are found primarily at lower slips since the mixed lubrication region is absent from this mapping procedure. The difference between the final runs of the full range (A) and reduced range (B) is shown in the lower-right graph of Fig. 8 and shows that the final state between the 2 procedures is identical over the reduced range of entrainment. Clearly, the final friction values measured above a U_e of 2.5 m/s after running-in do not depend on operation in a mixed lubrication region.

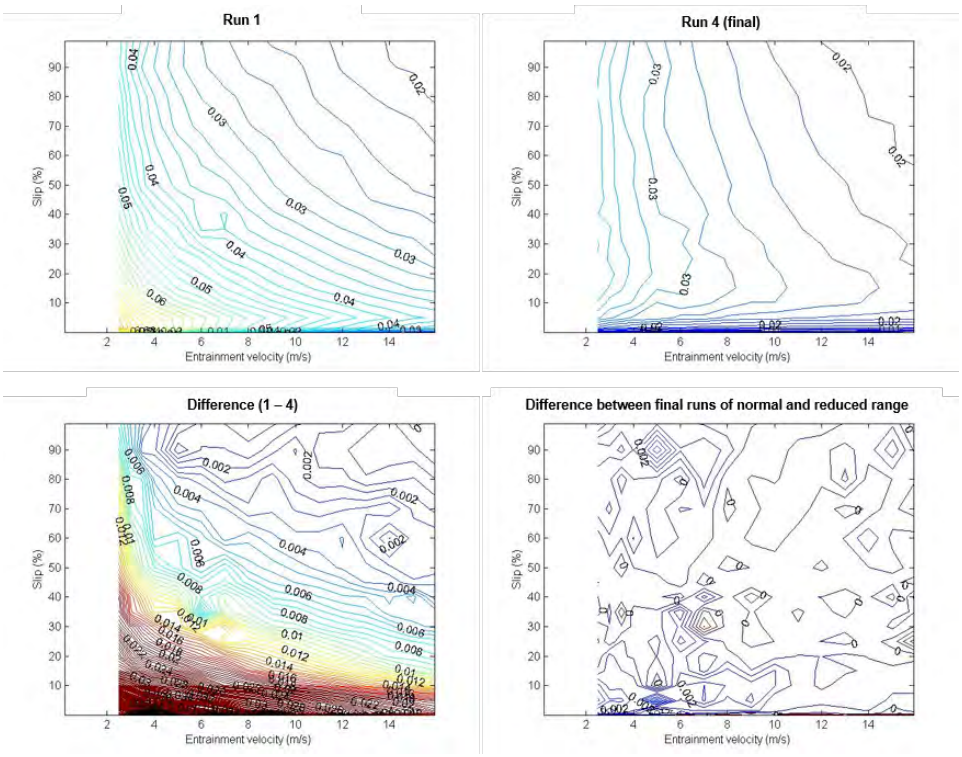

Fig. 8 First and last friction map using the ramp U_e, step slip procedure over a reduced U_e range (top), the difference between these maps (bottom left), and the difference between the final runs of the reduced range map and the full range map from Fig. 5 (bottom right)

3.4 Comparing Ramp Directions: Ramp Slip, Step U_e

The orientation of velocity ramp during the mapping procedure may result in a different running-in and a different final state. To explore whether such is the case, measurements were made over the same entrainment velocity-slip range as in the first mapping procedure, but in this case, the slip was ramped while the entrainment velocity was stepped (procedure C). The first run and last runs are shown in the top 2 graphs of Fig. 9. In run 1, the first ramp displays a transition from high friction coefficient to lower friction coefficient between the initial measurement point of high entrainment velocity and low slip and a higher slip of around 50% to 80%. This rapid transition does not occur again with later ramps, and the final run does not display such a transition. In the difference between the first and last runs in the lower graph of Fig. 9, this rapid transition is the largest change in friction during the running-in process. Otherwise, change in friction occurs throughout the full mapping area, but particularly at lower entrainment velocity weighted a bit toward lower slip. Interestingly, the change in friction becomes less at the lowest entrainment velocities below 0.75 m/s, which are the last to be measured in the initial run when compared to the ramps at around 1 to 2 m/s. This behavior is in contrast to that observed in procedure A.

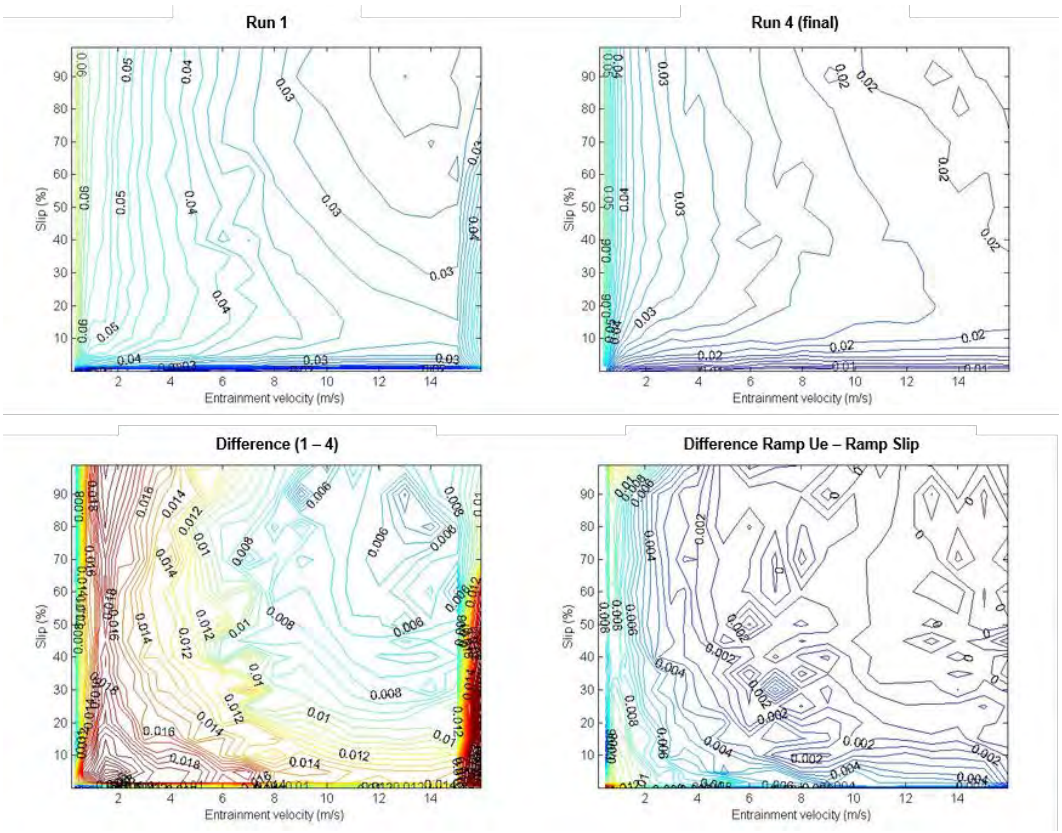

Fig. 9 First and last friction map using the ramp slip, step U_e procedure (top), the difference between these 2 maps (bottom left), and the difference between the final runs of the ramp slip map and the ramp U_e map from Fig. 5 (bottom right)

Overall, the change in friction occurs to a greater extent during the first run of this ramp slip mapping procedure and at higher entrainment velocities than procedure A (ramp U_e) earlier in the report. The rapid change during the initial ramp likely contributes significantly to the overall change, but this procedure also measures in the mixed lubrication region (low U_e) for a longer time than the first procedure. Also, the mixed lubrication regime is likely changing in its extent during the running-in procedure as roughness changes. Table 1 shows that this procedure spends nearly 3 times as long below a U_e of 2 m/s. The reason for the extended time spent in the mixed lubrication regime is to collect sufficiently spaced data points to capture the slope of the friction coefficient. The extended period of time spent in this regime may also be the reason that the running-in occurs largely before an entrainment velocity of less than 1 m/s is measured.

The difference between the last runs of the present mapping procedure C (ramp slip) and mapping procedure A (ramp U_e) is shown in the lower-right graph of Fig. 9. Here, the final state of running-in does depend on the ramp orientation, even for the same range. The friction coefficient is lower for procedure C (ramp

slip) than procedure A (ramp U_e) at low entrainment velocities and at low slips, although in the thermoviscous regime, the friction coefficient is equal between the two.

3.5 Constant Slip

Mapping out the friction coefficient over a large range of entrainment velocity and slip provides an excellent measure of general lubricant and surface properties, and the information gained can be correlated to gear tooth mesh behavior.[22] However, to accurately simulate the running-in for a gear tooth, a somewhat different procedure must be used. Any point along the gear tooth face in a spur gear contact will experience a single value of slip with the entrainment velocity changing as the gear is started, operated at various speeds, then stopped. To simulate this range of motion for a single point on the gear face (equivalent to a single point along the line of action in a gear mesh), a procedure was developed in which the entrainment velocity is ramped and the slip is held constant, procedure D.

The friction coefficient measured with entrainment velocity ramps at a constant slip of 95% is shown in Fig. 10 for a series of ramps. The first ramp begins at the lowest line in the bottom panel labeled Ramp 1 to 15, and each subsequent ramp is labeled with increasing ramp numbers moving upwards. Ramps 16 to 30 are found in the center panel, and Ramps 31 to 45 in the top panel. The friction coefficient decreases throughout the entire U_e range, but especially at lower U_e, from ramp to ramp. The decrease becomes less with each subsequent ramp and largely flattens out after 10 to 15 ramps, only decreasing slightly over the next 30 ramps. Interestingly, the first and the final ramps look similar to the first and the last measurements of the full mapping procedure in Fig. 5 when compared to the portion of the map at 95% slip. This ramping procedure at a single slip, however, takes more repetitions to come to a steadier final state than the other procedures.

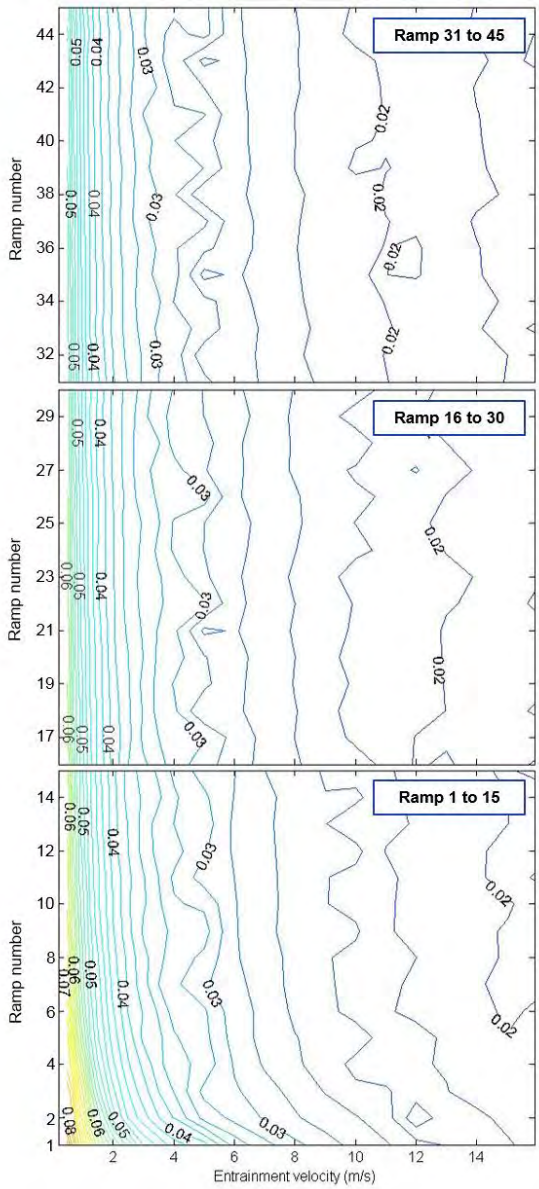

Fig. 10 Evolution of friction coefficient as a function of entrainment velocity and ramp number for the procedure ramp U_e at constant slip for ramp numbers 1 to 15 (bottom), 16 to 30 (center), and 31 to 45 (top)

3.6 Change in Surface Roughness

The process of running-in is typically considered to be a wear process that results in a smoother surface. By measuring the surface roughness with a 3-D profilometer, one can gauge both the change in roughness and the change in morphology. In Fig. 11, a 125- by 125-μm area of surface has been measured at the center of the track for the original as-ground surface and for each of the mapping procedures after the final state was reached. The original surface (top) displays ridges oriented from the upper left to the lower right. These ridges are the grinding marks from the machining of the disc surface and run in the circumferential direction always parallel to the measured track on the disc. Below the topology image of the original surface, the topologies after operation for each of the different mapping procedures are shown. They are strikingly similar in appearance to one another, and all display grooves remaining in the surface after the ridges have largely been displaced, either through plastic deformation or removal from the surface. The flattening of asperities is commonly seen in contact studies, even within the elastohydrodynamic lubrication (EHL) regime. Under the conditions of operation here, the grooves remaining on the surface seem to come from the deepest trenches between the ridges, as there are fewer grooves in the operated tracks than ridges on the pristine surface. Polishing of all but the deepest grooves is an indication that the conditions of operation here are severe enough to deform or remove a significant amount of material, but the wear process eventually reaches a limit at a particular smoothness of the surface.

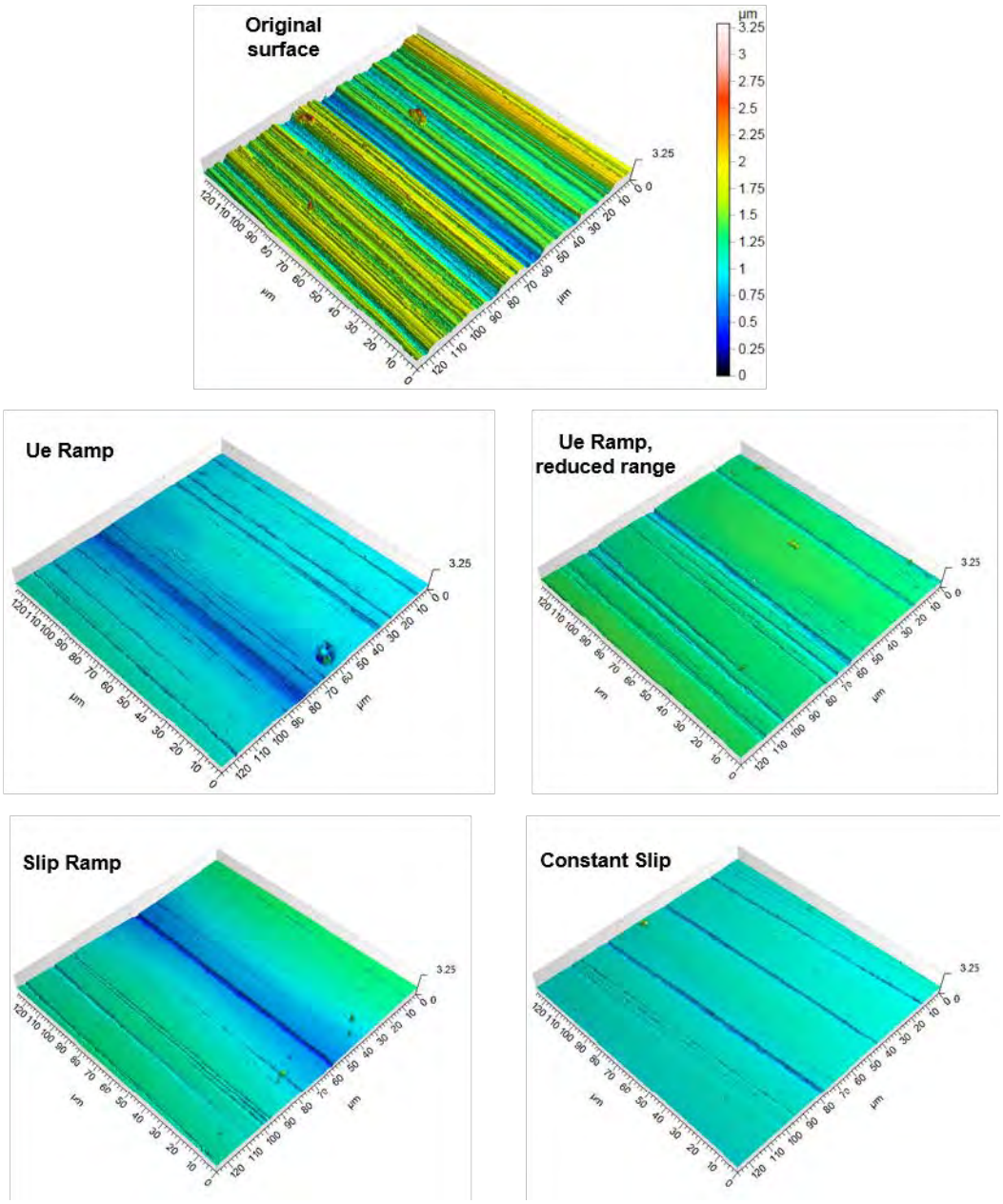

Fig. 11 Surface height plots (all same scale) from the original surface and the center of the track for each mapping procedure after the final mapping run

A statistical analysis of the surface roughness quantifies the similarities in the wear of the different mapping procedures and the limiting surface roughness. The wear tracks are roughly 400 to 500 µm wide and bend with a radius of 35 mm or greater circumferentially around the disc, so the roughness was measured over a 125- by 1,300-µm area centered on each track to capture a larger area of the track for analysis than that shown in Fig. 11. The roughness and height values calculated from these extended areas are given in Table 3. From the table, it can be seen that the original surface has a root mean square height S_q and average

height S_a of 0.278 and 0.218 μm, respectively. The operated surfaces average a bit less than half these amounts, and although there is a variation among the roughness, they all fall within 20% of the average S_q and 27% of the average S_a. Perhaps most telling is the valley height S_v of around 1.2 μm for all operated tracks that indicates a similar amount of loss of asperities for all procedures from the original S_v of 1.79 μm.

Table 3 Surface roughness (ISO 25178)

Procedure	S_q[a] (μm)	S_p[b] (μm)	S_v[c] (μm)	S_z[d] (μm)	S_a[e] (μm)
Original surface	0.278	2.70	1.79	4.49	0.218
Ramp U_e, step slip (A)	0.127	2.02	1.21	3.22	0.099
Ramp U_e (reduced range), step slip (B)	0.118	1.49	1.19	2.68	0.087
Ramp slip, step U_e (C)	0.148	2.18	1.13	3.31	0.119
Ramp U_e, constant slip (D)	0.099	2.35	1.22	3.56	0.070

[a] Root mean square (RMS) height of surface
[b] Maximum height of peaks
[c] Maximum height of valleys
[d] Maximum height of surface
[e] Arithmetical mean height of the surface

Among procedures, procedure C (ramp slip, step U_e) has the highest RMS and average roughness. Yet, unexpectedly, the friction coefficient for this procedure is equal to or lower than that of the other mapping procedures once the running-in process is complete. For higher entrainment velocities, both the final roughness and the direction of mapping do not have an effect on the friction coefficient (as evidenced by the nearly identical behavior) for the behavior above an entrainment velocity of 3 to 4 m/s of all procedures. The lower friction coefficient at low entrainment velocities for the ramp slip procedure must have its origin elsewhere than the roughness. The temperature profiles of the procedures differ, so one may consider that a drop in viscosity may be causing the lower friction. However, the temperature data are at odds with this hypothesis. Although the friction is lower for the ramp slip procedure across the entire low U_e region, the ramp slip procedure has an average contact temperature (average of ball and disc) of 106 °C across the entire low entrainment velocity region, while the ramp U_e procedure has an average temperature of 95 °C in the low slip, low U_e region and a temperature of 119 °C in the high slip, low U_e region. Further exploration is warranted to find the origin of the friction difference.

4. Conclusions

We have demonstrated the use of friction mapping to evaluate the process of running-in and its effects on EHL and mixed lubrication contacts. The main observations made during the operation of several different running-in procedures are as follows:

- The running-in process is more important for the mixed lubrication regime than for the EHL regime.
- The final state, once the running-in process is complete, of the friction coefficient and surface roughness over the mapped range of entrainment velocity and slip does not depend significantly on the ramp direction, nor on the particular range for those measured here.
- The friction coefficient does vary slightly between different ramp directions in the mixed lubrication regime.
- The surface morphology results in only the deepest grooves remaining with a very similar depth for all procedures.
- The running-in occurs at different rates and at different entrainment velocity and slip values, depending on the ramp direction and extent of mapping range. All maps contained ranges with a high slip at high entrainment velocity, but we did not determine whether this is the only requirement for running-in to the same extent.
- Heat generation depends much more on the particular contact operation conditions than on the amount of running-in, since the friction coefficient changes much less during running-in than the amount of power generation at different areas within the friction map.

Running-in is an important stage of operation for gear and bearing contacts that has a significant influence on their behavior over the life of the contact. This research establishes a basis for using friction mapping to determine the extent, rate, required contact conditions, and friction effect of the running-in process under relevant contact conditions for these components. These procedures may be used to explore the effects of contact pressure, temperature, lubricant chemistry, and contact material properties. They may also aid in development of running-in protocols for newly built transmissions, or even in the design of components to achieve a particular running-in during operation. Further, a period of running-in is typically conducted before evaluation of the particular parameters of interest during tribological and component testing to avoid confounding effects. Although

this period is normally conducted over the same period of time to provide the same amount of running-in among experiments, a deeper understanding of the process and its outcome under particular conditions can aid in selecting appropriate procedures.

5. References

1. Crook A. Simulated gear-tooth contacts: some experiments upon their lubrication and subsurface deformations. Proceedings of the Institution of Mechanical Engineers. 1957;171(1):187–214.
2. Tallian TE, Chiu YP, Huttenlocher DF, Kamenshine JA, Sibley LB, and Sindlinger NE. Lubricant films in rolling contact of rough surfaces. ASLE Transactions. 1964;7(2):109–126.
3. Ludema KC. A review of scuffing and running-in of lubricated surfaces, with asperities and oxides in perspective. Wear. 1984;100(1):315–331.
4. Dowson D, Taylor CM, Godet M, editors. The Running-In Process in Tribology: Proceedings of the 8th Leeds-Lyon Symposium on Tribology; 1981 Sep 8–11; Lyon, France. Surrey (UK): Butterworth and Co.; c1982.
5. Blau PJ. On the nature of running-in. Tribology International. 2006;38(11–12):1007–1012.
6. Berthe D, Flamand L, Foucher D, Godet M. Micropitting in Hertzian contacts. Journal of Lubrication Technology. 1980;102(4):478–489.
7. Zhou RS, Cheng HS, Mura T. Micropitting in rolling and sliding contact under mixed lubrication. Journal of Tribology. 1989;111(4):605–613.
8. Stout K, King T, Whitehouse D. Analytical techniques in surface topography and their application to a running-in experiment. Wear. 1977;43(1):99–115.
9. Wang F-X, Lacey P, Gates RS, Hsu SM. A study of the relative surface conformity between two surfaces in sliding contact. Journal of Tribology. 1991;113(4):755–761.
10. Chengwei W, Linqing Z. Effect of waviness and roughness on lubricated wear related to running-in. Wear. 1991;147(2):323–334.
11. Horng J-H, Len M-L, Lee J-S. The contact characteristics of rough surfaces in line contact during running-in process. Wear. 2002;253(9–10):899–913.
12. Zhu H, Ge S, Huang X, Zhang D, Liu J. Experimental study on the characterization of worn surface topography with characteristic roughness parameter. Wear. 2003;255(1–6):309–314.
13. Zhu H, Ge S, Cao X, Tang W. The changes of fractal dimensions of frictional signals in the running-in wear process. Wear. 2007;263(7–12):1502–1507.

14. Wang W, Wong P, Zhang Z. Experimental study of the real time change in surface roughness during running-in for PEHL contacts. Wear. 2000;244(1–2):140–146.

15. Lugt PM, Severt RWM, Fogelströ J, Tripp JH. Influence of surface topography on friction, film breakdown and running-in in the mixed lubrication regime. Proceedings of the Institution of Mechanical Engineers, Part J: Journal of Engineering Tribology. 2001;215(6):519–533.

16. Wang W, Wong P, Guo F. Application of partial elastohydrodynamic lubrication analysis in dynamic wear study for running-in. Wear. 2004;257(7–8):823–832.

17. Kupková M, Kupka M, Rudnayová E, Dusza J. On the use of fractal geometry methods for the wear process characterization. Wear. 2005;258(9):1462–1465.

18. Akbarzadeh S, Khonsari M. Experimental and theoretical investigation of running-in. Tribology International. 2011;44(2):92–100.

19. Björling M, Larsson R, Marklund P, Kassfeldt E. Elastohydrodynamic lubrication friction mapping – the influence of lubricant, roughness, speed, and slide-to-roll ratio. Proceedings of the Institution of Mechanical Engineers, Part J: Journal of Engineering Tribology. 2011;225(7):671–681.

20. Björling M, Isaksson P, Marklund P, Larsson R. The influence of DLC coating on EHL friction coefficient. Tribology Letters. 2012;47(2):285–294.

21. Björling M, Habchi W, Bair S, Larsson R. Marklund P. Towards the true prediction of EHL friction. Tribology International. 2013;66:19–26.

22. Björling M, Miettinen J, Marklund P, Lehtovaara A, Larsson R. The correlation between gear contact friction and ball on disc friction measurements. Tribology International. 2015;83:114–119.

23. Habchi W, Bair S, Vergne P. On friction regimes in quantitative elastohydrodynamics. Tribology International. 2013;58:107–117.

24. ISO 25178. Geometrical product specification (GPS) – surface texture: areal – part 70: material measures. Geneva (Switzerland): International Organization for Standardization; 2014.

List of Symbols, Abbreviations, and Acronyms

3-D	3-dimensional
AISI	American Iron and Steel Institute
EHL	elastohydrodynamic lubrication
ISO	International Organization for Standardization
RMS	root mean square
S_a	arithmetical mean height of the surface
S_p	maximum height of peaks
S_q	root mean square (RMS) height of surface
SRR	slide-to-roll ratio
S_v	maximum height of valleys
S_z	maximum height of surface
T_b	ball temperature
T_d	disc temperature
U_b	ball velocity at point of contact
U_d	disc velocity at point of contact
U_e	entrainment velocity
U_s	sliding velocity

1 (PDF)	DEFENSE TECHNICAL INFORMATION CTR DTIC OCA
2 (PDF)	DIRECTOR US ARMY RESEARCH LAB RDRL CIO LL IMAL HRA MAIL & RECORDS MGMT
1 (PDF)	GOVT PRINTG OFC A MALHOTRA
13 (9 PDF, 4 HC)	DIR USARL RDRL SER P AMIRTHARAJ RDRL SER E R DEL ROSARIO (HC) J WILSON J PENN (3 HC) R PROIE E VIVEIROS RDRL VT M VALCO K MORGAN RDRL VTP S BERKEBILE B DYKAS N MURTHY